Epstein-Barr virus tegument protein BGLF2 in exosomes released from virus-producer cells assists *de novo* infection

Yoshitaka Sato[1,2,#,*], Masahiro Yaguchi[1,#], Yusuke Okuno[3], Hanako Ishimaru[4], Somi Ozaki[1], Takeshi Suzuki[1], Tomoki Inagaki[1], Miki Umeda[1], Takahiro Watanabe[1], Masahiro Fujimuro[4], Takayuki Murata[1,5], Hiroshi Kimura[1,*]

[1]Department of Virology, Nagoya University Graduate School of Medicine, Nagoya 466-8550, Japan

[2]PRESTO, Japan Science and Technology Agency (JST), Kawaguchi 332-0012, Japan

[3]Pediatric Cancer Treatment Center, Nagoya University Hospital, Nagoya 466-8550, Japan

[4]Department of Cell Biology, Kyoto Pharmaceutical university, Kyoto 607-8412, Japan

[5]Department of Virology and Parasitology, Fujita Health University School of Medicine, Toyoake 470-1192, Japan

[#]These authors contributed equally to this study. Author order was determined alphabetically.

*To whom correspondence should be addressed:
Yoshitaka Sato (yssato@med.nagoya-u.ac.jp) and Hiroshi Kimura (hkimura@med.nagoya-u.ac.jp)

Running title: Exosomal transfer of tegument protein during infection

Keywords: EBV, exosome, BGLF2, de novo infection, extra-virus particle

Summary

Viruses must adapt to the environment of their host cells to establish infection and persist. Diverse mammalian cells, including virus-infected cells, secrete extracellular vesicles such as exosomes containing proteins and miRNAs, and use these vesicles to mediate intercellular communications. However, the roles of exosomes in viral infection remain unclear. Here we screened viral proteins to identify those responsible for the exosome-mediated upregulation of Epstein-Barr virus (EBV) infection. We found BGLF2 protein encapsulated in exosomes, which were released from EBV-infected cells. BGLF2 protein is a tegument protein that exists the space between the envelope and the nucleocapsid, and it is released into the cytoplasm shortly after infection. BGLF2 protein-containing exosomes enhanced viral gene expression and repressed innate immunity, thereby assisting the EBV infection. In summary, the EBV tegument protein BGLF2 is encapsulated not only encapsulated in viral particles, but also in exosomes secreted from infected cells. Therefore, BGLF2 may play a crucial role in establishing EBV latent infection.

43 **Introduction**

44 Epstein-Barr virus (EBV), a member of the herpesviruses, mainly infects B cells.
45 EBV infects about 90% of the world's population asymptomatically, but can cause
46 infectious mononucleosis and malignancies such as Burkitt lymphoma, T/NK cell
47 lymphoma, nasopharyngeal carcinoma, and gastric carcinoma (Cohen et al., 2011;
48 Young and Rickinson, 2004). EBV demonstrates a biphasic life cycle that includes a
49 latent phase and a lytic (productive replication) phase (Murata and Tsurumi, 2014).
50 After primary infection, although EBV preferentially remains latent in host cells without
51 viral production, a limited number of viral genes are expressed. Under certain
52 circumstances, latency is disrupted, and the virus shifts into the lytic phase. During this
53 productive replication phase, all >80 viral genes are expressed, the viral genome
54 undergoes replication, and progeny virions are produced (McKenzie and El-Guindy,
55 2015; Murata, 2014).

56 Similar to that of other herpesviruses, the EBV virion is composed of a viral
57 genomic DNA-containing nucleocapsid surrounded by a viral envelope with
58 glycoprotein spikes on its surface (Diefenbach, 2015; Knipe et al., 2007). Located
59 between the nucleocapsid and the outer viral envelope is the viral tegument which
60 includes >10 viral proteins called tegument proteins (Johannsen et al., 2004) that are
61 involved not only in morphogenesis, envelopment, and egress of progeny virions but
62 also in primary *de novo* infection (Sathish et al., 2012). Because they are released
63 shortly after infection into the cytoplasm, tegument proteins play major roles in
64 infectivity by modulating the intracellular environment. Indeed, we recently showed that
65 the EBV tegument protein BGLF2 increases viral infectivity (Konishi et al., 2018).

66 Extracellular vesicles such as exosomes are secreted from eukaryotic cells. These
67 vesicles can contain proteins, RNA, microRNA, or DNA, and they serve as crucial
68 mediators of intercellular communication involved in organismal homeostasis and
69 disease states (Raab-Traub and Dittmer, 2017; Record et al., 2014; Yanez-Mo et al.,
70 2015). The roles of extracellular vesicles have received considerable attention in recent
71 years. Exosomes secreted by virus-infected cells contain viral materials (Meckes and
72 Raab-Traub, 2011). Interestingly, EBV-infected cell lines secrete a higher number of
73 extracellular vesicles than uninfected cells (Hurwitz et al., 2017), leading us to

74 hypothesize that EBV utilizes exosomes to influence infection and pathogenesis by
75 facilitating viral replication or activating immune evasion strategies. For instance, the
76 viral oncoprotein latent membrane protein 1 (LMP1) has been detected in exosomes
77 (Houali et al., 2007; Sato et al., 2017; Vazirabadi et al., 2003). LMP1-positive
78 exosomes activate the extracellular signal-regulated kinase and phosphoinositide 3-
79 kinase (PI3K)/Akt signaling pathways in the recipient cells (Meckes et al., 2010).
80 Although EBV encodes more than 80 genes, many of which are lytic proteins, the
81 majority of viral proteins detected in exosomes are latent proteins (Zhao et al., 2019),
82 because these latent proteins have been identified using a forward genetics approach.
83 Therefore, it is still unclear which EBV lytic proteins are encapsulated in exosomes and
84 function during infection.
85 In this study, we use a reverse genetics approach to investigate the role of EBV
86 protein-containing exosomes during infection. We performed a series of screenings
87 and identified the tegument protein BGLF2, which enhanced *de novo* infection via
88 exosomes. Our results suggest that this tegument protein functions via extracellular
89 vesicle transfer like that of virus particles, ensuring efficient and robust modulation of
90 the microenvironment for the infection.
91
92 **Results**
93 ***Screening for EBV proteins that modulate infection via exosomal transfer***
94 To explore the roles of exosomes containing EBV proteins during infection, we
95 generated an exosome library, from 293T cells expressing 71 different epitope-tagged
96 EBV lytic proteins (Konishi et al., 2018), and screened for EBV genes that both
97 modulated infection and were detected in exosomes (Figure 1A). EBV-negative
98 Akata(-) B-cells treated with each exosome from the library were experimentally
99 infected with EBV, and the infectivity at 48 h post-infection (hpi) was compared (Figure
100 1B, upper panel). Additionally, the exosome library was subjected to immunoblot
101 analysis with an anti-hemagglutinin (HA) antibody to detect EBV proteins in the
102 exosomes (Figure 1B, lower panel). By integrating multiple screenings, we found
103 BGLF2 and BLRF1 within exosomes, and that they enhanced EBV infection. Because

104 BLRF1 encodes envelope glycoprotein N, which localized to the membrane, we here
105 focus on the tegument protein BGLF2.
106
107 ***Exosome-mediated release of BGLF2 in culture supernatant***
108 Because exosomes were purified by a precipitation-based method in our screening
109 for easy handling, we could not rule out the possibility of non-exosome contamination
110 (Patel et al., 2019). To examine the incorporation of BGLF2 in the exosomes, we
111 isolated exosomes, using an affinity-based method, from the culture supernatant of
112 293T cells expressing BGLF2-HA. BGLF2 was also detected in the exosomes purified
113 by both exosome-affinity resin (Figure 2A) and anti-CD9 antibody (data not shown).
114 Size range and morphology of exosomes were characterized via nanoparticle tracking
115 analysis (NTA) and transmission electron microscopy (TEM), respectively (Figure 2B
116 and C). We confirmed that cellular cytochrome C (Yoshioka et al., 2013) could not be
117 detected in the purified exosomes, suggesting no contamination of any other types
118 (Figure 2D). Moreover, we confirmed that the detergent treatment of the culture
119 supernatant impeded the BGLF2 detection in the exosomes, suggesting that BGLF2
120 was encapsulated within the exosomes (Figure 2E).
121 BGLF2 stimulates the activator protein (AP)-1 signaling pathway (Konishi et al.,
122 2018; Liu and Cohen, 2016). To assess the function of BGLF2-containing exosomes,
123 we added them to cells that were transfected with a pAP-1-Luc reporter and control
124 plasmids. As shown in Figure 2F, BGLF2 was taken up by the recipient cells, and
125 treatment with BGLF2-containing exosomes enhanced AP-1 reporter activity (Figure
126 2G). GW4869, a compound blocking exosome release by neutral sphingomyelinase
127 inhibition (Trajkovic et al., 2008), prevented AP-1 activation (Figure 2G). These findings
128 indicate that functional BGLF2 is transferred via exosomes to recipient cells.
129 We further evaluated whether BGLF2-containing exosomes could be released from
130 infected cells. Conditioned medium from lytic-induced Akata/EBV-EGFP cells by IgG
131 was subjected to floating density gradient ultracentrifugation and separated into 18
132 fractions (Figure 3A). Each fraction was characterized by immunoblotting with exosome
133 marker antibodies and quantitative polymerase chain reaction (qPCR) analysis for EBV
134 genome detection (Figure 3B). Three fractions containing exosomes (E), virions (V),

135 and control (C) were pooled and further evaluated as the antibody against BGLF2 did
136 not exhibit high sensitivity. As shown in Figures 3C and D, BGLF2 proteins were
137 detected in pool E, which was free of viral genome and viral capsid antigen (VCA),
138 indicating that infected cells released BGLF2-containing exosomes during the lytic
139 replication.
140
141 ***EBV BGLF2 orthologs of in herpes simplex virus-1 and human cytomegalovirus***
142 ***are incorporated into exosomes***
143 To define the regions of BGLF2 responsible for packaging into exosomes, we
144 created truncation mutants of BGLF2, which is 336 amino acids (aa) in length, and
145 then tested each for its incorporation (Supplementary Figure S1A). Bortezomib, a
146 proteasome inhibitor, was used for stabilizing deletion mutants. As shown in Figure
147 S1A, the deletion of 98-158 aa precluded the incorporation of BGLF2 into exosomes,
148 although deletion of the C-terminal domain did not. Thus, the incorporation of BGLF2
149 into exosomes required its central domain. In line with previous reports (Cai et al.,
150 2017; Salsman et al., 2008), BGLF2 exhibited a pan-cellular localization pattern without
151 a restricted colocalization with CD63, a marker for multi-vesicular bodies
152 (Supplementary Figure S1B).
153 All herpesviruses possess a BGLF2 homologue (Liu and Cohen, 2016). Therefore,
154 we tested whether the orthologs of EBV BGLF2 such as herpes simplex virus type 1
155 (HSV-1) UL16 and human cytomegalovirus (HCMV) UL94 proteins were incorporated
156 into exosomes. HSV-1 UL16 and HCMV UL94 proteins were detected in exosomes
157 purified from cells expressing HSV-1 UL16 and HCMV UL94 (Figure 4). These findings
158 indicate a conserved role of exosomes containing BGLF2 or its herpesviral orthologs
159 proteins.
160
161 ***Extra-virion particle BGLF2 enhances the infectivity of BGLF2-KO EBV***
162 Next, we examined whether exosomal-transferred BGLF2 supports infection of
163 using a BGLF2-knockout (BGLF2-KO) EBV. The knockout of BGLF2 reduces EBV
164 infectivity upon *de novo* infection of B-cells (Konishi et al., 2018). Treatment with

165 exosomes containing BGLF2 significantly enhanced the infectivity of BGLF2-KO EBV
166 compared with a control treatment (Figure 5A).
167 To evaluate the effect of BGLF2-containing exosomes on EBV infection, we
168 performed RNA-seq analysis (Figure 5B). Akata(-) cells were pre-treated with BGLF2-
169 containing exosomes or control exosomes and then infected with BGLF2-KO EBV. We
170 collected infected cells by fluorescence-activated cell sorting (FACS) at 24 hpi
171 according to EGFP-positivity, and performed RNA-seq to obtain transcriptome
172 information. As shown in Figure 5C and 5D, treatment with BGLF2-containing
173 exosomes induced expression of EBV genes, although the expression level of EGFP,
174 which was driven from a eukaryotic promoter (Delecluse et al., 1998), was the same.
175 This enhanced EBV mRNA expression was validated using qPCR (Figure 5E). LMP1
176 was one of the most significantly expressed viral genes between the groups treated
177 with exosomes with or without BGLF2 (Figure 5C).
178 Among down-regulated genes following treatment with BGLF2-containing
179 exosomes, the terms “Toll-like receptor signaling” and “cytosolic DNA-sensing” were
180 enriched by DAVID analysis (Huang da et al., 2009) of RNA-seq data (Figure 5F). This
181 is consistent with a recent report that ORF33, the ortholog of BGLF2 in Kaposi’s
182 sarcoma-associated herpesvirus (KSHV), suppresses the interferon (IFN) beta
183 production pathway for immune evasion (Yu et al., 2020). Consequently, we
184 investigated whether BGLF2-containing exosomes modulated the innate immune
185 response. Polyinosinic-polycytidylic acid [poly(I:C)] was used to stimulate the TLR3-
186 mediated IFN beta production pathway (Takeuchi and Akira, 2010). As shown in Figure
187 5G, BGLF2-containing exosomes inhibited IFN beta mRNA expression under poly(I:C)
188 stimulation. We confirmed that type I IFNs inhibited EBV infection in a dose-dependent
189 manner (Figure 5H).
190 Together, our data indicate that BGLF2 is encapsulated not only encapsulated in
191 viral particles, but also in exosomes secreted from infected cells. BGLF2 delivered via
192 exosomes promotes optimal EBV infection by enhancing viral gene expression and
193 repressing innate immunity (Figure 5I).
194
195

196 **Discussion**

197 Virally infected cells release virions as infectious particles and non-infectious
198 particles. All herpesvirus-infected cells are known to release L-particles in addition to
199 virions (Chang et al., 1997; Granato et al., 2008; Irmiere and Gibson, 1983). L-particles
200 are non-infectious because they are composed of the virus envelope and tegument
201 proteins but lack viral genome and nucleocapsid proteins. This conserved release of L-
202 particles may shed light on an essential role of non-infectious particles in creating a
203 microenvironment that facilitates their replication, spread, and persistence in the host
204 cells. Recently, it was shown that L-particles mediate immune evasion by CD83 down-
205 modulation on mature dendritic cells (Heilingloh et al., 2015).

206 BGLF2 protein impairs type I IFN signaling through Tyk2 (Liu et al., 2020) and also
207 dampens NF-κB activity (Chen et al., 2019) in a cell-dependent manner during lytic
208 infection. Expression of KSHV ORF33 (the ortholog of BGLF2) suppresses the IFN
209 beta production pathway (Yu et al., 2020). Here, we demonstrated that exsosomal
210 tegument protein BGLF2 was transferred to the target cells and in turn enhanced EBV
211 infectivity by manipulating the cellular environment (Figure 5I). BGLF2 delivered via
212 exosomes increase the expression of EBV genes (Figure 5C-E). The LMP1 expression
213 is upregulated by the binding of AP-1 with CCAAT enhancer binding proteins (C/EBPs)
214 on its promoter (Noda et al., 2011). The EBV gene BHRF1 is highly expressed during
215 the first two days after infection (Mrozek-Gorska et al., 2019; Wang et al., 2019). These
216 findings imply a role for BGLF2 in viral gene expression in infected cells, consistent
217 with previous reports that BGLF2 activates p38, JNK, and AP-1 to induce viral gene
218 expression (Konishi et al., 2018; Liu and Cohen, 2016). Furthermore, exosomes
219 prepared from BGLF2-expressing 293T cells inhibited IFN beta production stimulation
220 (Figure 5G), protecting infected cells from a type I IFN-mediated response during *de*
221 *novo* infection. Exosomal BGLF2 protein was active in the recipient cells (Figure 2G
222 and 4) suggesting that exosomes serve as a carrier of herpesvirus tegument proteins
223 to target cells. Indeed, BGLF2-containing exosomes were released from EBV-infected
224 cells that lytically produced infectious virions (Figure 3).

225 EBV can hijack and use extracellular vesicles such as exosomes. It is known that
226 EBV increases the extracellular vesicle secretion (Hurwitz et al., 2017) and EBV

227 miRNAs delivered via exosomes increase the severity of EBV-mediated
228 lymphoproliferative disease (Higuchi et al., 2018). Although exosomes are released in
229 exocytic bursts upon the fusion of the multivesicular bodies to the cell membrane
230 (Colombo et al., 2014), the final envelopment site for EBV is the Golgi apparatus
231 (Nanbo et al., 2018), indicating that these non-infectious particles (L-particles and
232 exosomes) are generated in non-Golgi compartments. Furthermore, BGLF2 and its
233 orthologs in HSV-1 and HCMV were incorporated into exosomes (Figure 4), indicating
234 that manipulation of the cellular environment by exosomes is a conserved mechanism
235 among herpesvirus. The results of this study also suggest a previously unforeseen
236 essential role for non-infectious particles in viral protection.
237
238 **Materials and Methods**
239 ***Cells, plasmids and reagents***
240 HEK293T (ATCC CRL-3216) and HEK293/EBV(dBGLF2) cells (Konishi et al.,
241 2018) were maintained in DMEM supplemented with 10% fetal bovine serum (FBS).
242 Akata(−) (Shimizu et al., 1994), and Akata/EBV-EGFP (Masud et al., 2017) cells were
243 cultured in RPMI1640 medium containing 10% FBS. AGS/EBV-EGFP cells (a kind gift
244 from Hironori Yoshiyama) (Katsumura et al., 2009) were grown in F-12 HAM's medium
245 supplemented with 10% FBS and 400 μg/mL G418.
246 The BZLF1-expression plasmid and HA-tagged EBV lytic protein-expression library
247 were described previously (Konishi et al., 2018; Sato et al., 2009). For expression of C-
248 terminal HA-tagged HSV-1 UL16 and HCMV UL94, constructs expressing UL16 and
249 UL94 in pcDNA3 (Thermo Fisher Scientific, Waltham, MA, USA) were prepared by
250 PCR and the In-Fusion cloning system (Takara Bio, Kusatsu, Shiga, Japan). The
251 inserted DNA sequence of each vector was confirmed by direct DNA sequencing. The
252 reporter plasmid pAP1-Luc and promoterless-RLuc (pGL4.70) were purchased from
253 Promega (Madison, WI, USA).
254 Bortezomib (Cat# A10160; AdooQ BioScience, Irvine, CA, USA) was used at a
255 concentration of 100 nM. Recombinant human type I IFN alpha (Cat# 11200-1) and
256 IFN beta (Cat# 11415-1) were purchased from PBL Assay Science (Piscataway, NJ,
257 USA). For inhibition of exosome secretion, cells were treated with 10 μM GW4869

258 (Cat# 13127; Cayman Chemical, Ann Arbor, MI, USA). Transient transfection of
259 poly(I:C) (Cat# 4287/10; R&D Systems, Minneapolis, MN, USA) was performed with
260 Lipofectamine 2000 (Thermo Fisher Scientific) according to the manufacturer's
261 protocol.
262
263 ***Antibodies and immunoblotting***
264 Anti-HA (3F10) rat antibody was purchased from Sigma-Aldrich (St. Louis, MO,
265 USA). Anti-CD63 (Ts63) mouse and anti-VCA (PA1-73003) goat antibodies were
266 obtained from Thermo Fisher Scientific. Rabbit anti-GAPDH (14C10), rabbit anti-CD9
267 (D8O1A), and horseradish peroxidase-conjugated secondary antibodies were
268 purchased from Cell Signaling Technology (Danvers, MA, USA). Anti-CD81 (5A6)
269 mouse antibody was obtained from Santa Cruz Biotechnology (Dallas, TX, USA).
270 Antiserum against EBV BGLF2 was prepared by immunizing a rabbit with the synthetic
271 peptide NH2-CAHVNILRGWTEDDSPGTS-COOH, and the serum was purified by
272 affinity purification using the same peptide (Cosmo Bio, Tokyo, Japan) (Supplementary
273 Figure S2). Immunoblot and signal detection were performed as described previously
274 (Sato et al., 2009).
275
276 ***Virus preparation***
277 EGFP-EBV was obtained from the 8-day-old cell-free supernatant of AGS/EGFP-
278 EBV cells. The cell-free supernatant was filtered through 0.45 μm filters and then used
279 as a virus stock. For the preparation of the BGLF2-KO virus, HEK293/EBV(dBGLF2)
280 cells (Konishi et al., 2018) were transfected with BZLF1 expression plasmid using
281 Lipofectamine 2000 (Thermo Fisher Scientific) according to the manufacturer's
282 instructions. Cells and media were harvested and freeze-thawed, and cell debris was
283 removed. The supernatant after centrifugation was filtered through 0.45 μm filters and
284 then used as a virus stock. EBV-negative Akata(-) cells were infected with the virus,
285 and EGFP-positive cells were counted by FACS to measure the viral titer.
286
287 ***Exosome purification***
288 Exosome-containing conditioned media were centrifuged at 2000 × g to remove
289 cells. Exosomes were purified with a Total Exosome Isolation Kit (Thermo Fisher

290 Scientific) for screenings or exoEasy Maxi Kit (Qiagen, Hilden, Germany) according to
291 the manufacturer's protocols.
292 Size and particle number were analyzed using the LM10 or NS300 nanoparticle
293 characterization system (NanoSight; Malvern Panalytical, Worcestershire, United
294 Kingdom).
295
296 ***Transmission electron microscopy (TEM)***
297 For negative staining TEM analysis, the samples were absorbed on formvar film
298 coated copper grids and were stained with 2% phosphotungstic acid solution (pH 7.0)
299 for 1 min. The grids were observed using a transmission microscope (JEM-1400Plus;
300 JEOL Ltd., Tokyo, Japan) at an acceleration voltage of 100 kV. Digital images were
301 captured using a CCD camera (EM-14830RUBY2; JEOL Ltd.).
302
303 ***Floating density gradient ultracentrifugation***
304 Semi-confluent Akata/EBV-eGFP cells were washed with PBS twice and
305 suspended in medium containing EV-free FBS and anti-human IgG for the induction of
306 lytic replication. After 72 h, 100 ml of the conditioned medium was centrifuged at 1,500
307 g and 4°C for 5 min to remove cells and debris. The supernatant was filtered by using a
308 0.45-μm filter (Merck, Darmstadt, Germany) and extracellular vesicles including
309 exosomes and virions were pelleted by ultracentrifugation at 141,000 g at 4 °C for 2 h
310 in a swinging-bucket rotor (SW28; Beckman Coulter, Brea, CA, USA). The pellet was
311 resuspended in filtered PBS and centrifuged at 18,300 g and 4°C for 10 min to remove
312 insoluble aggregates. The supernatant was mixed with iodixanol (Optiprep;
313 Cat#1114542, Cosmo Bio) (40% (w/v) final concentration of iodixanol). A discontinuous
314 iodixanol gradient was prepared as following: sample/iodixanol was applied to the
315 bottom of the tube, followed by 35%, 30%, 25%, and 20% (w/v) iodixanol/PBS, covered
316 by 15% (w/v) iodixanol/PBS. The density gradient centrifugation was performed at
317 141,000 g and 4 °C for 20 h in a SW28 swing rotor (Beckman Coulter). A total of 18
318 fractions were collected starting from the top.
319
320 ***Screenings***

321 HEK293T cells were transfected with each plasmid expressing an EBV gene using
322 Lipofectamine 2000 (Thermo Fisher Scientific). On the following day, media were
323 changed to DMEM supplemented with 5% exosome-depleted FBS (System
324 Biosciences, Palo Alto, CA, USA). After 48 h, exosomes were purified from the
325 conditioned media. To identify exosomal proteins, we analyzed purified exosomes by
326 immunoblot. For analyzing modulators of infectivity, EBV-negative Akata(-) cells were
327 treated with purified exosomes in RPMI1640 supplemented with 5% exosome-depleted
328 FBS (System Biosciences, Palo Alto, CA, USA). After 6 h, cells were infected with
329 EGFP-EBV. At 48 h after infection, cells were fixed with 4% paraformaldehyde. The
330 infectivity was determined using a flow cytometer (FACS Canto, BD Biosciences, San
331 Jose, CA, USA).
332
333 ***Luciferase reporter assay***
334 HEK293T cells were transfected with AP-1 reporter plasmid (pAP1-Luc) and
335 promoterless-RLuc as an internal control using Lipofectamine 2000 (Thermo Fisher
336 Scientific) and incubated in DMEM supplemented with 5% exosome-depleted FBS.
337 After 48 h, cells were treated with purified exosome. Cells were lysed 24 h later and
338 subjected to luciferase assays using the Dual-Luciferase Reporter Assay System
339 (Promega).
340
341 ***RNA-seq***
342 Akata(-) cells were pre-treated with BGLF2-containing or control exosome for 16 h,
343 and then infected with BGLF2-KO EBV at room temperature for 2 h with agitation. After
344 infection, cells were resuspended in medium containing exosomes. The top 30,000
345 EBV-infected cells expressing EGFP were sorted by a FACS Aria II Cell Sorter (BD
346 Biosciences) at 24 hpi.
347 Total RNA was extracted using the RNeasy Mini kit (Qiagen). Evaluation of RNA,
348 RNA-seq library preparation, Illumina sequencing, and data preprocessing were
349 performed as described previously (Okuno et al., 2019).
350
351 ***qPCR***

352 Total RNA was reverse-transcribed to cDNA using the PrimeScript II Reverse
353 transcriptase kit (Takara Bio) or the *SuperPrep* II Cell Lysis & RT kit for qPCR (TOYOBO,
354 Osaka, Japan). Viral DNA and mRNA levels were analyzed by qPCR using the 7500
355 Fast DX Real-Time PCR system (Applied Biosystems, Foster City, CA, USA) as
356 previously described (Sato et al., 2017). The primer sequences used in this study are
357 listed in Table 1.
358
359 ***Statistical analysis***
360 Results are shown as the means ± standard error (SE) of at least three independent
361 experiments. Statistical analyses were performed using Microsoft Excel. Welch's t-test
362 was used to determine significance, and $P < 0.05$ was considered to be statistically
363 significant.
364
365 ***Data availability***
366 All RNA-seq datasets have been deposited to the DNA Data Bank of Japan (DDBJ;
367 https://www.ddbj.nig.ac.jp/index-e.html) under the accession number: DRA010388.
368
369 **Acknowledgements**
370 The authors thank Hironori Yoshiyama for providing invaluable materials; Yohei
371 Yamauchi for comments on the manuscript; Daisuke Yuasa, Shingo Ochiai, Shuko
372 Kumagai, and Tomoko Kunogi for technical supports; Minoru Tanaka and the Division
373 for Medical Research Engineering, Nagoya University Graduate School of Medicine for
374 FACS analysis.
375 This work was supported in part by grants from the Japan Society for the Promotion
376 of Science (JSPS) KAKENHI (https://www.jsps.go.jp) (Grant Numbers JP19H04829,
377 JP21K15448 to Y.S., and JP20H03493 to H.K.); the JST (https://www.jst.go.jp)
378 PRESTO (Grant Number JPMJPR19H5) to Y.S.; the Japan Agency for Medical
379 Research and Development (AMED, https://www.amed.go.jp) (JP19fm0208016 and
380 JP20wm0325012 to T.M., JP19ck0106517 to Y.O., and JP19jk0210023 to Y.S.); the
381 Takeda Science Foundation (https://www.takeda-sci.or.jp) to Y.S. and T.M.; the Hori
382 Sciences and Arts Foundation (https://www.hori-foundation.or.jp) to Y.S. and H.K.; the

383 MSD Life Science Foundation (https://www.msd-life-science-foundation.or.jp) to Y.S.;
384 and the Uehara Memorial Foundation (https://www.ueharazaidan.or.jp/) to H.K.. H.I. is
385 supported by the JSPS Research fellowship (19J23589). T.S. and T.I. are supported
386 by the Takeda Science Foundation scholarship.
387

388 **Declaration of interests**

389 The authors declare no competing interests.

390

391 **References**

392 Cai, M., Liao, Z., Chen, T., Wang, P., Zou, X., Wang, Y., Xu, Z., Jiang, S., Huang, J., Chen, D.*, et*
393 *al.* (2017). Characterization of the subcellular localization of Epstein-Barr virus encoded proteins
394 in live cells. Oncotarget *8*, 70006-70034.
395 Chang, Y.E., Van Sant, C., Krug, P.W., Sears, A.E., and Roizman, B. (1997). The null mutant of
396 the U(L)31 gene of herpes simplex virus 1: construction and phenotype in infected cells. J Virol
397 *71*, 8307-8315.
398 Chen, T., Wang, Y., Xu, Z., Zou, X., Wang, P., Ou, X., Li, Y., Peng, T., Chen, D., Li, M.*, et al.*
399 (2019). Epstein-Barr virus tegument protein BGLF2 inhibits NF-kappaB activity by preventing
400 p65 Ser536 phosphorylation. FASEB J *33*, 10563-10576.
401 Cohen, J.I., Fauci, A.S., Varmus, H., and Nabel, G.J. (2011). Epstein-Barr virus: an important
402 vaccine target for cancer prevention. Sci Transl Med *3*, 107fs107.
403 Colombo, M., Raposo, G., and Thery, C. (2014). Biogenesis, secretion, and intercellular
404 interactions of exosomes and other extracellular vesicles. Annu Rev Cell Dev Biol *30*, 255-289.
405 Delecluse, H.J., Hilsendegen, T., Pich, D., Zeidler, R., and Hammerschmidt, W. (1998).
406 Propagation and recovery of intact, infectious Epstein-Barr virus from prokaryotic to human
407 cells. Proc Natl Acad Sci U S A *95*, 8245-8250.
408 Diefenbach, R.J. (2015). Conserved tegument protein complexes: Essential components in the
409 assembly of herpesviruses. Virus Res *210*, 308-317.
410 Djavadian, R., Hayes, M., and Johannsen, E. (2018). CAGE-seq analysis of Epstein-Barr virus
411 lytic gene transcription: 3 kinetic classes from 2 mechanisms. PLoS Pathog *14*, e1007114.
412 Granato, M., Feederle, R., Farina, A., Gonnella, R., Santarelli, R., Hub, B., Faggioni, A., and
413 Delecluse, H.J. (2008). Deletion of Epstein-Barr virus BFLF2 leads to impaired viral DNA
414 packaging and primary egress as well as to the production of defective viral particles. J Virol *82*,
415 4042-4051.
416 Heilingloh, C.S., Kummer, M., Muhl-Zurbes, P., Drassner, C., Daniel, C., Klewer, M., and
417 Steinkasserer, A. (2015). L Particles Transmit Viral Proteins from Herpes Simplex Virus 1-

418 Infected Mature Dendritic Cells to Uninfected Bystander Cells, Inducing CD83
419 Downmodulation. J Virol *89*, 11046-11055.
420 Higuchi, H., Yamakawa, N., Imadome, K.I., Yahata, T., Kotaki, R., Ogata, J., Kakizaki, M., Fujita,
421 K., Lu, J., Yokoyama, K.*, et al.* (2018). Role of exosomes as a proinflammatory mediator in the
422 development of EBV-associated lymphoma. Blood *131*, 2552-2567.
423 Houali, K., Wang, X., Shimizu, Y., Djennaoui, D., Nicholls, J., Fiorini, S., Bouguermouh, A., and
424 Ooka, T. (2007). A new diagnostic marker for secreted Epstein-Barr virus encoded LMP1 and
425 BARF1 oncoproteins in the serum and saliva of patients with nasopharyngeal carcinoma. Clin
426 Cancer Res *13*, 4993-5000.
427 Huang da, W., Sherman, B.T., and Lempicki, R.A. (2009). Systematic and integrative analysis of
428 large gene lists using DAVID bioinformatics resources. Nat Protoc *4*, 44-57.
429 Hurwitz, S.N., Nkosi, D., Conlon, M.M., York, S.B., Liu, X., Tremblay, D.C., and Meckes, D.G.,
430 Jr. (2017). CD63 Regulates Epstein-Barr Virus LMP1 Exosomal Packaging, Enhancement of
431 Vesicle Production, and Noncanonical NF-kappaB Signaling. J Virol *91*, e02251-02216.
432 Irmiere, A., and Gibson, W. (1983). Isolation and characterization of a noninfectious virion-like
433 particle released from cells infected with human strains of cytomegalovirus. Virology *130*, 118-
434 133.
435 Johannsen, E., Luftig, M., Chase, M.R., Weicksel, S., Cahir-McFarland, E., Illanes, D., Sarracino,
436 D., and Kieff, E. (2004). Proteins of purified Epstein-Barr virus. Proc Natl Acad Sci U S A *101*,
437 16286-16291.
438 Katsumura, K.R., Maruo, S., Wu, Y., Kanda, T., and Takada, K. (2009). Quantitative evaluation
439 of the role of Epstein-Barr virus immediate-early protein BZLF1 in B-cell transformation. J Gen
440 Virol *90*, 2331-2341.
441 Knipe, D., Howley, P., Griffin, D., Lamb, R., Martin, M., Roizman, B., and Straus, S. (2007).
442 Fields Virology, 5th edn (Philadelphia: Lippincott Williams & Wilkins).
443 Konishi, N., Narita, Y., Hijioka, F., Masud, H., Sato, Y., Kimura, H., and Murata, T. (2018).
444 BGLF2 Increases Infectivity of Epstein-Barr Virus by Activating AP-1 upon De Novo Infection.
445 mSphere *3*, e00138-00118.
446 Liu, X., and Cohen, J.I. (2016). Epstein-Barr Virus (EBV) Tegument Protein BGLF2 Promotes
447 EBV Reactivation through Activation of the p38 Mitogen-Activated Protein Kinase. J Virol *90*,
448 1129-1138.
449 Liu, X., Sadaoka, T., Krogmann, T., and Cohen, J.I. (2020). Epstein-Barr Virus (EBV)
450 Tegument Protein BGLF2 Suppresses Type I Interferon Signaling To Promote EBV
451 Reactivation. J Virol *94*, e00258-00220.

452 Masud, H., Watanabe, T., Yoshida, M., Sato, Y., Goshima, F., Kimura, H., and Murata, T.
453 (2017). Epstein-Barr Virus BKRF4 Gene Product Is Required for Efficient Progeny Production.
454 J Virol *91*, e00975-00917.
455 McKenzie, J., and El-Guindy, A. (2015). Epstein-Barr Virus Lytic Cycle Reactivation. Curr Top
456 Microbiol Immunol *391*, 237-261.
457 Meckes, D.G., Jr., and Raab-Traub, N. (2011). Microvesicles and viral infection. J Virol *85*,
458 12844-12854.
459 Meckes, D.G., Jr., Shair, K.H., Marquitz, A.R., Kung, C.P., Edwards, R.H., and Raab-Traub, N.
460 (2010). Human tumor virus utilizes exosomes for intercellular communication. Proc Natl Acad
461 Sci U S A *107*, 20370-20375.
462 Mrozek-Gorska, P., Buschle, A., Pich, D., Schwarzmayr, T., Fechtner, R., Scialdone, A., and
463 Hammerschmidt, W. (2019). Epstein-Barr virus reprograms human B lymphocytes immediately
464 in the prelatent phase of infection. Proc Natl Acad Sci U S A *116*, 16046-16055.
465 Murata, T. (2014). Regulation of Epstein-Barr virus reactivation from latency. Microbiol
466 Immunol *58*, 307-317.
467 Murata, T., and Tsurumi, T. (2014). Switching of EBV cycles between latent and lytic states.
468 Rev Med Virol *24*, 142-153.
469 Nanbo, A., Noda, T., and Ohba, Y. (2018). Epstein-Barr Virus Acquires Its Final Envelope on
470 Intracellular Compartments With Golgi Markers. Front Microbiol *9*, 454.
471 Noda, C., Murata, T., Kanda, T., Yoshiyama, H., Sugimoto, A., Kawashima, D., Saito, S.,
472 Isomura, H., and Tsurumi, T. (2011). Identification and characterization of CCAAT enhancer-
473 binding protein (C/EBP) as a transcriptional activator for Epstein-Barr virus oncogene latent
474 membrane protein 1. J Biol Chem *286*, 42524-42533.
475 Okuno, Y., Murata, T., Sato, Y., Muramatsu, H., Ito, Y., Watanabe, T., Okuno, T., Murakami,
476 N., Yoshida, K., Sawada, A.*, et al.* (2019). Defective Epstein-Barr virus in chronic active
477 infection and haematological malignancy. Nat Microbiol *4*, 404-413.
478 Patel, G.K., Khan, M.A., Zubair, H., Srivastava, S.K., Khushman, M., Singh, S., and Singh, A.P.
479 (2019). Comparative analysis of exosome isolation methods using culture supernatant for
480 optimum yield, purity and downstream applications. Sci Rep *9*, 5335.
481 Raab-Traub, N., and Dittmer, D.P. (2017). Viral effects on the content and function of
482 extracellular vesicles. Nat Rev Microbiol *15*, 559-572.
483 Record, M., Carayon, K., Poirot, M., and Silvente-Poirot, S. (2014). Exosomes as new vesicular
484 lipid transporters involved in cell-cell communication and various pathophysiologies. Biochim
485 Biophys Acta *1841*, 108-120.

Salsman, J., Zimmerman, N., Chen, T., Domagala, M., and Frappier, L. (2008). Genome-wide screen of three herpesviruses for protein subcellular localization and alteration of PML nuclear bodies. PLoS Pathog *4*, e1000100.

Sathish, N., Wang, X., and Yuan, Y. (2012). Tegument Proteins of Kaposi's Sarcoma-Associated Herpesvirus and Related Gamma-Herpesviruses. Front Microbiol *3*, 98.

Sato, Y., Kamura, T., Shirata, N., Murata, T., Kudoh, A., Iwahori, S., Nakayama, S., Isomura, H., Nishiyama, Y., and Tsurumi, T. (2009). Degradation of Phosphorylated p53 by Viral Protein-ECS E3 Ligase Complex. PLoS Pathog *5*, e1000530.

Sato, Y., Ochiai, S., Murata, T., Kanda, T., Goshima, F., and Kimura, H. (2017). Elimination of LMP1-expressing cells from a monolayer of gastric cancer AGS cells. Oncotarget *8*, 39345-39355.

Shimizu, N., Tanabe-Tochikura, A., Kuroiwa, Y., and Takada, K. (1994). Isolation of Epstein-Barr virus (EBV)-negative cell clones from the EBV-positive Burkitt's lymphoma (BL) line Akata: malignant phenotypes of BL cells are dependent on EBV. J Virol *68*, 6069-6073.

Takeuchi, O., and Akira, S. (2010). Pattern recognition receptors and inflammation. Cell *140*, 805-820.

Trajkovic, K., Hsu, C., Chiantia, S., Rajendran, L., Wenzel, D., Wieland, F., Schwille, P., Brugger, B., and Simons, M. (2008). Ceramide triggers budding of exosome vesicles into multivesicular endosomes. Science *319*, 1244-1247.

Vazirabadi, G., Geiger, T.R., Coffin, W.F., 3rd, and Martin, J.M. (2003). Epstein-Barr virus latent membrane protein-1 (LMP-1) and lytic LMP-1 localization in plasma membrane-derived extracellular vesicles and intracellular virions. J Gen Virol *84*, 1997-2008.

Wang, C., Li, D., Zhang, L., Jiang, S., Liang, J., Narita, Y., Hou, I., Zhong, Q., Zheng, Z., Xiao, H.*, et al.* (2019). RNA Sequencing Analyses of Gene Expression during Epstein-Barr Virus Infection of Primary B Lymphocytes. J Virol *93*, e00226-00219.

Yanez-Mo, M., Siljander, P.R., Andreu, Z., Zavec, A.B., Borras, F.E., Buzas, E.I., Buzas, K., Casal, E., Cappello, F., Carvalho, J.*, et al.* (2015). Biological properties of extracellular vesicles and their physiological functions. J Extracell Vesicles *4*, 27066.

Yoshioka, Y., Konishi, Y., Kosaka, N., Katsuda, T., Kato, T., and Ochiya, T. (2013). Comparative marker analysis of extracellular vesicles in different human cancer types. J Extracell Vesicles *2*.

Young, L.S., and Rickinson, A.B. (2004). Epstein-Barr virus: 40 years on. Nat Rev Cancer *4*, 757-768.

Yu, K., Tian, H., and Deng, H. (2020). PPM1G restricts innate immune signaling mediated by STING and MAVS and is hijacked by KSHV for immune evasion. Sci Adv *6*.

Zhao, M., Nanbo, A., Sun, L., and Lin, Z. (2019). Extracellular Vesicles in Epstein-Barr Virus' Life Cycle and Pathogenesis. Microorganisms *7*, 48.

522

523

524 **Figure Legends**

525

526 **Figure 1: Combined screenings for the viral proteins that regulate the infectivity**
527 **via exosomal transfer.**

528 (A) The workflow of the screenings. Exosomes were purified from the conditioned
529 media of HEK293T cells that were transfected with each plasmid expressing an EBV
530 gene. For analyzing modulators of infectivity, EBV-negative Akata(-) cells were pre-
531 treated with purified exosomes and then infected with EGFP-EBV. The infectivity was
532 determined at 48 hpi by FACS analysis. For identifying exosomal proteins, purified
533 exosomes were analyzed by immunoblot with an anti-HA antibody.

534 (B) Heatmap showing fold change (FC) of infectivity of EBV with Akata(-) cells in the
535 presence of each exosome at 48 hpi. Infectivity changes (top panel) reflect the $\log^2$ FC
536 relative to the control exosome purified from empty vector-transfected cells. p values
537 are shown on the middle panel. The viral protein in purified exosomes is indicated as
538 black on the bottom panel.

539

540

541 **Figure 2: Functional BGLF2 proteins are transferred to the recipient cells via**
542 **exosomes.**

543 (A) BGLF2 protein-containing exosomes were secreted from BGLF2-expressing cells.
544 HEK293T cells were transfected with HA-tagged BGLF2-expression or empty plasmid.
545 Exosomes were isolated from the supernatant of the cells. CD63 and CD9 served as
546 exosome markers.

547 (B) TEM image of the exosomes purified from BGLF2-expressing HEK293T cells.
548 Scale bar represents 100 nm.

549 (C) NanoSight profiles showing size distribution for exosomes purified from BGLF2-
550 expressing HEK293T cells.

551 (D) Western blot results showing the absence or underrepresentation of negative
552 exosome marker cytochrome-C (Cyt *c*) in isolated exosomes.

553 (E) BGLF2 protein was incorporated into exosomes. Exosomes were purified from
554 supernatants treated with or without 0.25% Triton-X 100 for 5 min at room temperature.

555 (F) BGLF2 was delivered to the recipient cells via exosomes. HEK293T cells were
556 treated with BGLF2-containing exosomes for the indicated number of hours and then
557 washed extensively and harvested. Cell lysates were applied to immunoblot analysis.
558 (G) BGLF2 transferred via exosomes activated the AP-1 promoter. Exosomes were
559 purified from HEK293T cells transfected with BGLF2-expression plasmid or empty
560 plasmid in the presence or absence of GW4869. HEK293T cells transfected with the
561 pAP-1-Luc and promoterless-Rluc plasmids, and then treatment with BGLF2-
562 containing exosomes. Cell lysates were obtained at 24 h post-treatment and analyzed
563 using luciferase reporter assays. Values (mean ± SEs) were calculated from three
564 independent experiments. Asterisks, $p<0.05$; n.s., not significant.
565
566
567 **Figure 3: BGLF2-containing exosomes are released from infected cells.**
568 (A) Centrifugation protocol and workflow for separation and enrichment of exosomes
569 and virions.
570 (B) Exosome marker proteins were enriched in fractions #1-3 after iodixanol floating
571 density gradient centrifugation. For the Western blotting analysis, proteins in each
572 fraction were concentrated by acetone precipitation. CD63 and CD81 served as
573 exosome markers. The EBV genome in each fraction was quantified by qPCR.
574 (C) and (D) Pool E (fraction #1-3) containing the BGLF2 protein. Each pool (E, fraction
575 #1-3; V, fractions #5-6; and C, fractions #14-16) was analyzed by qPCR (C) and
576 Western blot (D). Data are presented as the means ± SE. Viral capsid antigen (VCA)
577 p18 served as virion marker.
578
579
580 **Figure 4: The orthologs of BGLF2 are incorporated into exosomes**
581 HEK293T cells were transfected with expression plasmids containing HA-tagged
582 BGLF2 or its HSV-1 or HCMV orthologs. Exosomes were isolated from the supernatant
583 of the cells.
584
585

586 **Figure 5: BGLF2-containing exosomes enhance the infectivity of BGLF2-KO EBV.**
587 (A) Akata(-) cells were infected with BGLF2-KO EBV in the presence of BGLF2-
588 containing exosomes. After two days, GFP positivity was determined by FACS. Results
589 are presented as means ± SE of at least three independent experiments and are shown
590 as relative infectivity to control treatment with PBS (infectivity value of 1). Double
591 asterisks, $p<0.01$; n.s., not significant.
592 (B) The workflow of sample collection for RNA-seq/qRT-PCR analyses. Akata(-) cells
593 were pre-treated with exosomes for 16 h, and then infected with BGLF2-KO EBV. The
594 infected cells were collected via FACS at 24 hpi. Total RNA extracted from the sorted
595 cells was subjected to RNA-seq and qRT-PCR.
596 (C) Gene expression levels were normalized as counts per million followed by $\log_2$-
597 transformation with a pseudo-count of 1. Each bar indicates the $\log_2$ fold change of a
598 viral gene expression between treatment with exosomes with or without BGLF2. Viral
599 gene expression kinetics are categorized into five groups: latent, immediate early,
600 early, leaky late, and late (Djavadian et al., 2018).
601 (D) Read counts of EBV genes in BGLF2-KO EBV-infected cells that were treated with
602 BGLF2-containing or control exosomes by RNA-seq.
603 (E) Validation of enhanced EBV gene expression by qPCR. Data are presented as
604 means ± SE. Samples were tested in duplicate. Asterisk, $p<0.05$; double asterisks,
605 $p<0.01$; n.s., not significant.
606 (F) DAVID analysis of RNA-seq data from BGLF2-KO EBV-positive cells treated with
607 BGLF2-containing or control exosomes. FDR; false discovery rate.
608 (G) HEK293 cells were treated with BGLF2-containing exosomes for 16 h. Cells were
609 challenged with transfection of poly(I:C) (2 μg/ml) for 2.5 h. RT-qPCR was conducted.
610 Data are presented as the means ± SE from three independent experiments. Asterisk,
611 $p<0.05$; n.s., not significant.
612 (H) Type I IFN inhibited EBV infection. Akata(-) cells were infected with EBV-EGFP in
613 the presence of IFN alpha and beta (100 or 500 Unit/mL). After two days, GFP
614 positivity was determined by FACS. Results are presented as means ± SE of three
615 independent experiments. Double asterisks, $p<0.01$; n.s., not significant.
616 (I) BGLF2 protein in exosomes cooperates with the tegument protein in the virions to
617 optimize the cellular condition for EBV infection. The tegument protein BGLF2 is

618 incorporated into both exosomes and virions. BGLF2-containing exosomes are
619 released from infected cells and transferred to the recipient cells.
620
621
622 **Supplementary Figure S1: The internal region of BGLF2 is required for**
623 **packaging into exosomes.**
624 (A) The C-terminal domain of BGLF2 was dispensable for incorporation into exosomes.
625 HEK293 cells were transfected with a deletion mutant of BGLF2-expression plasmids
626 and treated with or without 250 nM of Bortezomib for 24 h before harvest. Exosomes
627 were isolated from the culture supernatant.
628 (B) Cellular localization of BGLF2 and CD63 in HEK293 cells. HEK293 cells were
629 transfected with HA-tagged BGLF2-expression plasmid. Cells were fixed at 2 days
630 post-transfection and then stained with anti-HA and anti-CD63 antibodies.
631
632
633 **Supplementary Figure S2: Detection of BGLF2 protein by anti BGLF2 antibody.**
634 HEK293/EBV-dBGLF2 cells were transfected with the BZLF1- and HA-tagged BGLF2-
635 expression plasmids. Cells were harvested after 2 days and subjected to Western
636 blotting with anti-BGLF2, anti-BZLF1, anti-BMRF1, and anti-GAPDH antibodies.
637

638 **Table 1: Oligonucleotide primers used for qPCR**

639

Primer name	Sequence (5' to 3')
BALF2 forward	GCCCGTCCGGTTGTCA
BALF2 reverse	GGCCACGCTGATAAAGTTGTC
BHRF1 forward	AAATGGTACCCTGCATCCTG
BHRF1 reverse	CCACATGTTCGGTGTGTGTT
LMP1 forward	CTGATGATCACCCTCCTGCT
LMP1 reverse	CTAAGACAAGTAAGCACCCGAAG
EGFP forward	ACGTAAACGGCCACAAGTTC
EGFP reverse	AAGTCGTGCTGCTTCATGTG
GAPDH forward	CCTCCAAGGAGTAAGACCCC
GAPDH reverse	TGTGAGGAGGGGAGATTCAG
IFN beta forward	TGCTCTCCTGTTGTGCTTCTCC
IFN beta reverse	ATAGATGGTCAATGCGGCGT

640

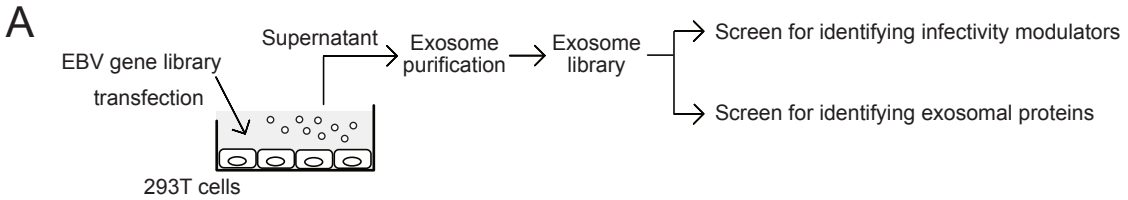
A
EBV gene library
transfection
293T cells
Supernatant
Exosome purification
Exosome library
Screen for identifying infectivity modulators
Screen for identifying exosomal proteins

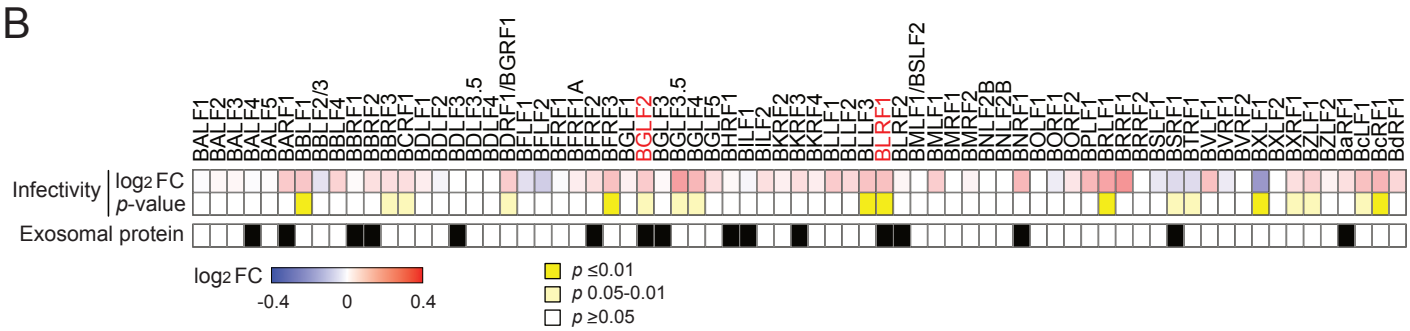
B
BALF1
BALF2
BALF3
BALF4
BALF5
BARF1
BBLF2/3
BBLF4
BBRF1
BBRF2
BBRF3
BCRF1
BDLF1
BDLF2
BDLF3
BDLF3.5
BDLF4
BDRF1/BGRF1
BFLF1
BFLF2
BFRF1
BFRF1A
BFRF2
BFRF3
BGLF1
BGLF2
BGLF3
BGLF3.5
BGLF4
BGLF5
BHRF1
BILF1
BILF2
BKRF2
BKRF3
BKRF4
BLLF1
BLLF2
BLLF3
BLRF1
BLRF2
BMLF1/BSLF2
BMLF1
BMRF1
BMRF2
BNLF2B
BNLF2B
BNRF1
BOLF1
BORF1
BORF2
BPLF1
BRLF1
BRRF1
BRRF2
BSLF1
BSRF1
BTRF1
BVLF1
BVRF1
BVRF2
BXLF1
BXLF2
BXRF1
BZLF1
BZLF2
BaRF1
BcLF1
BcRF1
BdRF1
Infectivity
log2 FC
p-value
Exosomal protein
log2 FC
-0.4
0
0.4
p ≤0.01
p 0.05-0.01
p ≥0.05

Sato and Yaguchi et al., Figure 2

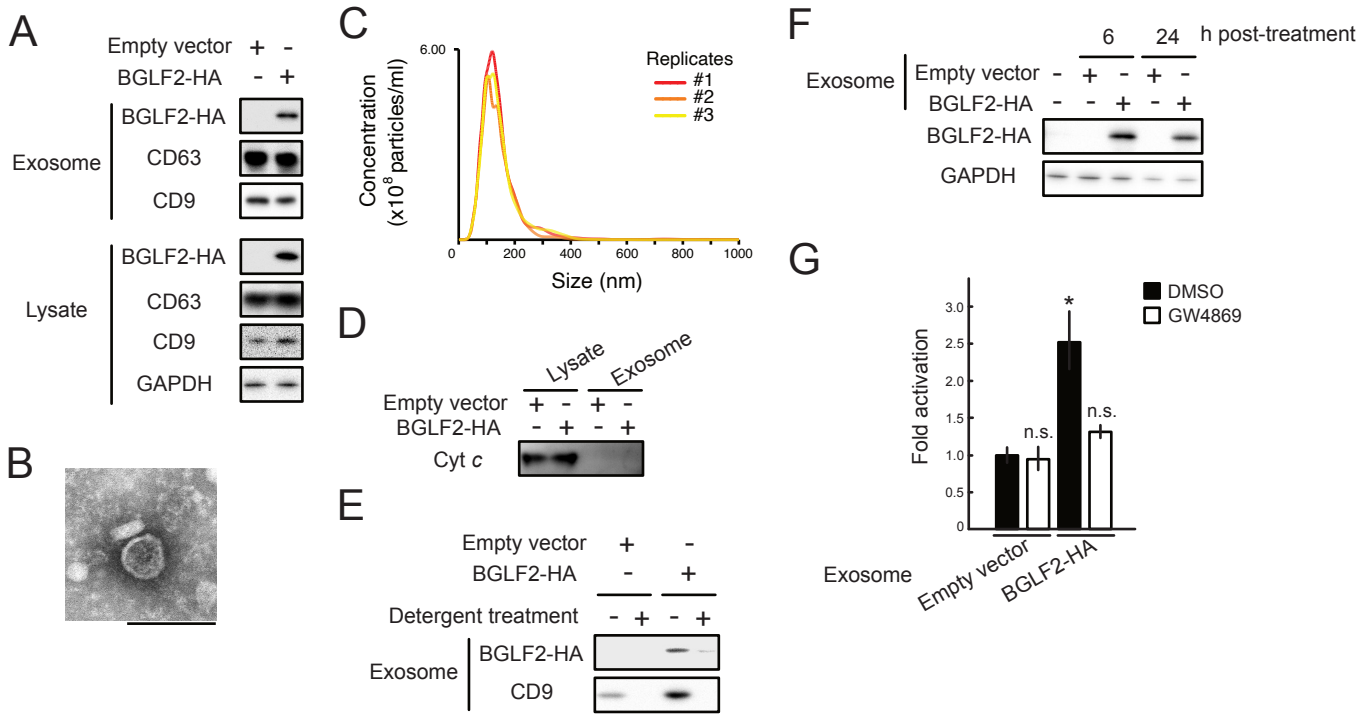

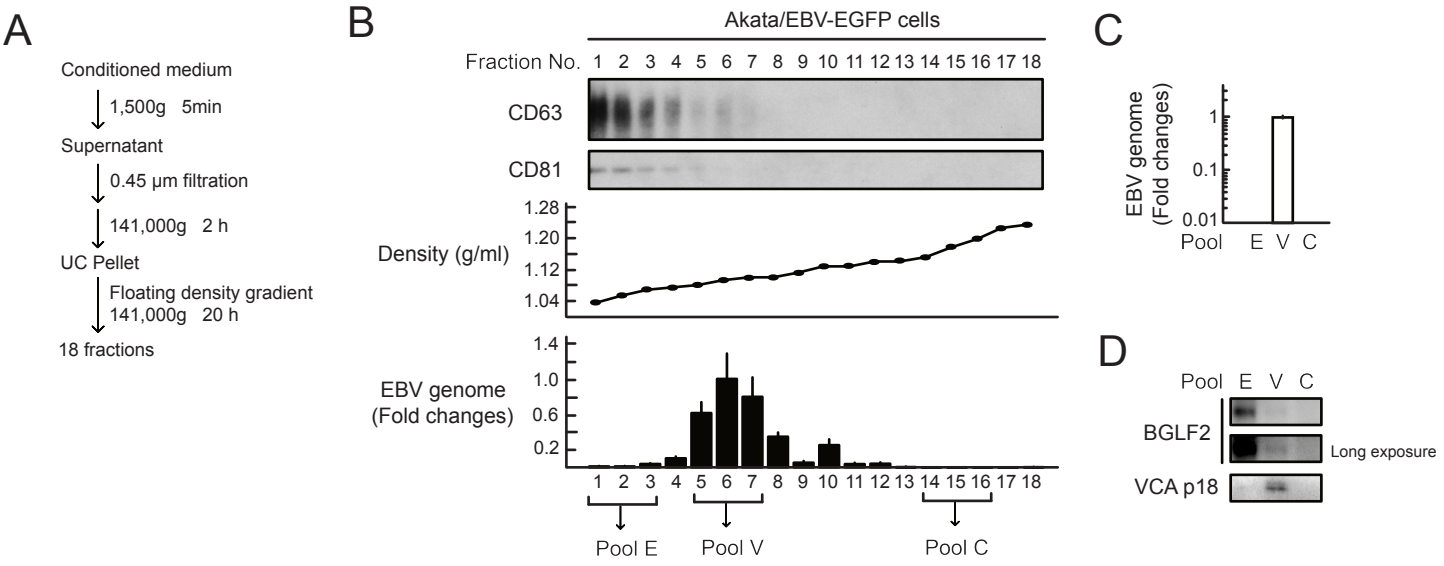
A
Conditioned medium
1,500g 5min
Supernatant
0.45 μm filtration
141,000g 2 h
UC Pellet
Floating density gradient
141,000g 20 h
18 fractions
B
Akata/EBV-EGFP cells
Fraction No. 1 2 3 4 5 6 7 8 9 10 11 12 13 14 15 16 17 18
CD63
CD81
Density (g/ml)
1.28
1.20
1.12
1.04
EBV genome
(Fold changes)
1.4
1.0
0.6
0.2
Pool E
Pool V
Pool C
C
EBV genome
(Fold changes)
1
0.1
0.01
Pool E V C
D
Pool E V C
BGLF2
Long exposure
VCA p18

Sato and Yaguchi et al., Figure 4

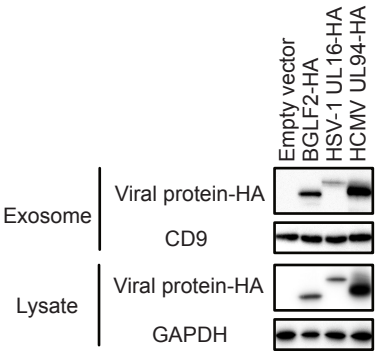

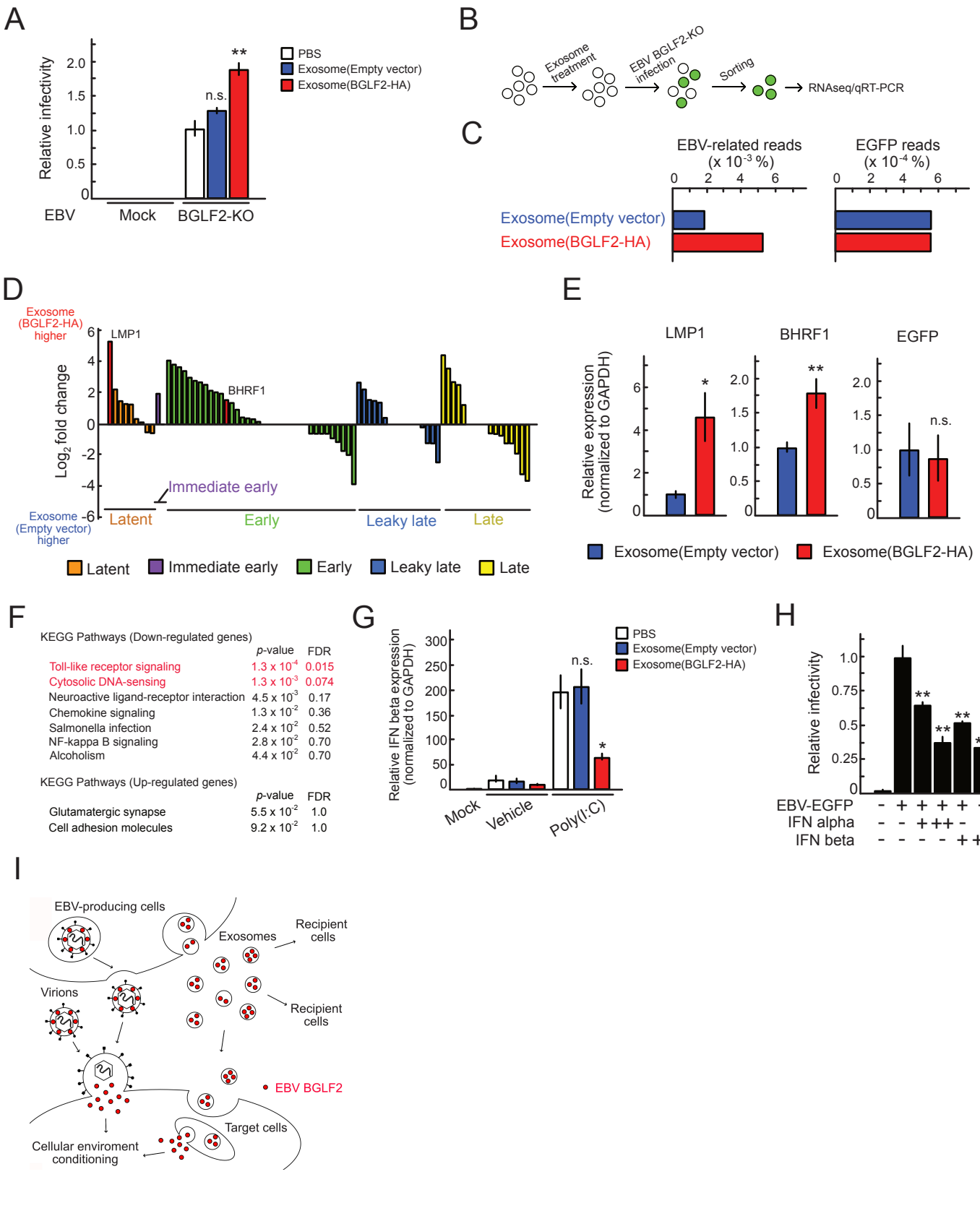
A
Relative infectivity
2.0
1.5
1.0
0.5
0
**
n.s.
PBS
Exosome(Empty vector)
Exosome(BGLF2-HA)
EBV
Mock
BGLF2-KO
B
Exosome treatment
EBV BGLF2-KO infection
Sorting
RNAseq/qRT-PCR
C
EBV-related reads (x 10-3 %)
EGFP reads (x 10-4 %)
0 2 4 6
Exosome(Empty vector)
Exosome(BGLF2-HA)
D
Exosome (BGLF2-HA) higher
Exosome (Empty vector) higher
Log2 fold change
LMP1
BHRF1
Immediate early
Latent
Early
Leaky late
Late
Latent
Immediate early
Early
Leaky late
Late
E
LMP1
BHRF1
EGFP
Relative expression (normalized to GAPDH)
*
**
n.s.
Exosome(Empty vector)
Exosome(BGLF2-HA)
F
KEGG Pathways (Down-regulated genes)
p-value FDR
Toll-like receptor signaling 1.3 x 10-4 0.015
Cytosolic DNA-sensing 1.3 x 10-3 0.074
Neuroactive ligand-receptor interaction 4.5 x 10-3 0.17
Chemokine signaling 1.3 x 10-2 0.36
Salmonella infection 2.4 x 10-2 0.52
NF-kappa B signaling 2.8 x 10-2 0.70
Alcoholism 4.4 x 10-2 0.70
KEGG Pathways (Up-regulated genes)
p-value FDR
Glutamatergic synapse 5.5 x 10-2 1.0
Cell adhesion molecules 9.2 x 10-2 1.0
G
Relative IFN beta expression (normalized to GAPDH)
300
250
200
150
100
50
0
n.s.
*
PBS
Exosome(Empty vector)
Exosome(BGLF2-HA)
Mock
Vehicle
Poly(I:C)
H
Relative infectivity
1.0
0.75
0.5
0.25
0
**
EBV-EGFP - + + + + +
IFN alpha - - +++ - -
IFN beta - - - - +++
I
EBV-producing cells
Exosomes
Recipient cells
Virions
Recipient cells
EBV BGLF2
Target cells
Cellular enviroment conditioning

Sato and Yaguchi et al., Supplementary Figure S1

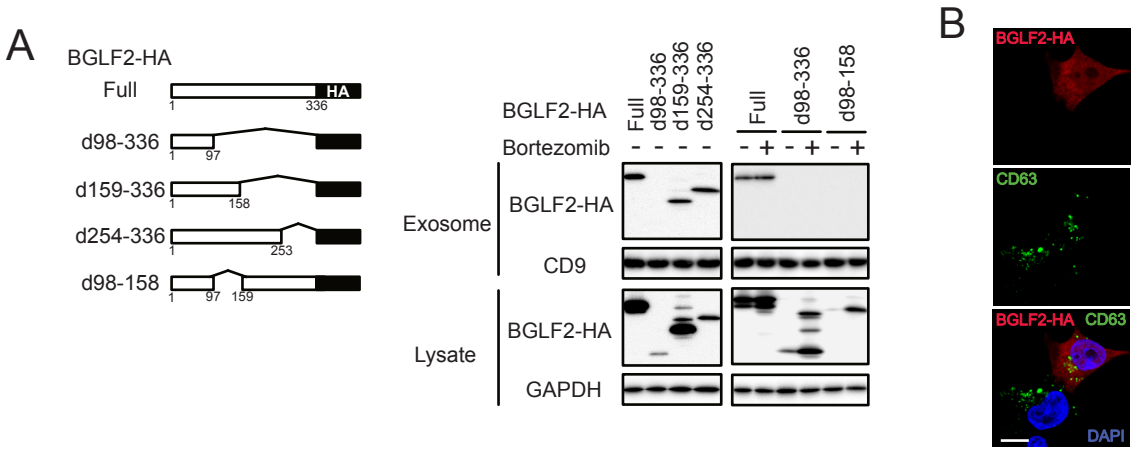
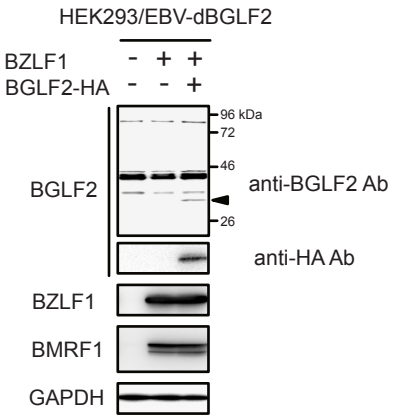
Sato and Yaguchi et al., Supplementary Figure S2